Available online at www.sciencedirect.com
SCIENCE DIRECT®
PERGAMON
Polyhedron 22 (2003) 1641–1644
POLYHEDRON
www.elsevier.com/locate/poly

Synthesis, molecular structure and electrochemical studies of the bis(diphenylphosphino)amine bridge triangular nickel clusters

Eugenio Simón-Manso, Peter Gantzel, Clifford P. Kubiak *

Department of Chemistry and Biochemistry, University of California, San Diego, CA 92093-0358, USA

Received 7 January 2003; accepted 24 March 2003

Abstract

The synthesis of the triangular trinuclear nickel complexes ($[Ni_3(\mu\text{-}I)_2(\mu\text{-}dppa)_3]^{+n}$, $n = 0, +1$; dppa = ligand bis(diphenylphosphine)amine), is reported. The crystallographic study of these clusters allows a detailed structural comparison with the bis(diphenylphosphine)methane (dppm) analogs. Differences in electrochemical redox potentials are discussed in the light of stronger metal–phosphorus interaction in the dppa clusters. The dppa clusters $[Ni_3(\mu\text{-}I)_2(\mu\text{-}dppa)_3]^{+}$, show a larger HOMO–LUMO gap, denoting greater thermodynamic stability of the dppa bridged $51e^-$ species, compared to its dppm analog.
© 2003 Elsevier Science Ltd. All rights reserved.

Keywords: Bis(diphenylphosphino)amine; Bis(diphenylphosphino)methane; Nickel cluster

1. Introduction

The transition-metal chemistry of bis(diphenylphosphino)amine (dppa) $NR(PPh_2)_2$ (R = H, Me, Ph) has developed rapidly in recent years due to its versatile coordination properties. In a manner similar to that of the widely used bis(diphenylphosphino)methane (dppm, $CH(PPh_2)_2$) these phosphinoamine ligands can bind to metal atoms in different ways: monodentate, chelating or bridging [1,2].

Farrar and coworkers [3] have suggested that the substitution of the methylene group in dppm with the smaller NH group may increase the ligand's propensity to bridge two metal atoms.

In previous reports, we have described dppm stabilized triangular nickel clusters that are electrocatalysts for CO_2 reduction [4,6a–d]. The presence of an acidic amine proton in a dppa ligand opens several synthetic opportunities beyond those available with dppm. For example, it is possible to perform template synthesis on a coordinated dppa ligand [7]. In particular, treatment of primary amines with PCl_3 or Ph_2PCl allows the facile introduction of a range of possible substituents at the nitrogen atom, and this is a versatile and cost effective synthetic route for diphosphinoamines [2]. In this communication we report the synthesis, X-ray characterization and electrochemical studies of new trinuclear nickel complexes stabilized with dppa.

2. Experimental

$Ni(COD)_2$ and dppa were synthesized according to reported procedures [5,2b]. All reactions were carried out inside a dry box. ^1H and ^{31}P NMR spectra were obtained in toluene-d_8 using a Varian Mercury 400 spectrometer. ^1H spectra are referenced to internal solvent peaks; ^{31}P NMR signals are reported with respect to external 85% H_3PO_4. MALDI Mass spectra were recorded at Scripps Research Institute (La Jolla, CA) mass spectrometry facility. Electrochemical measurements were performed on a BAS analytical instrument, using Pt working electrode and ferrocenium/ferrocene $[Cp_2Fe^+/Cp_2Fe]$ as a reference electrode, having +0.36 V difference with respect to SCE in our conditions. Density functional calculations were done using the hybrid functional of Becke [10a] with Perdew

* Corresponding author. Address: Department of Chemistry and Biochemistry, University of California, San Diego, 4223A Pacific Hall 9500 Gilman Drive, La Jolla, CA 92093-0332, USA. Tel.: +1-858-822-2655; fax: +1-858-534-5383.
E-mail address: ckubiak@ucsd.edu (C.P. Kubiak).

0277-5387/03/$ - see front matter © 2003 Elsevier Science Ltd. All rights reserved.
doi:10.1016/S0277-5387(03)00266-3

and Wang correlation [10b], using the LANL2DZ basis set (b3pw91/LanL2DZ) as implemented in GAUSSIAN-98 [10c]. The X-ray structure geometries were used as input and hydrogen atoms position were reoptimized.

2.1. $Ni_3(\mu^2\text{-dppa})_3(\mu^3\text{-I})_2$ (1)

This complex has been synthesized by modifying methods [4] for the synthesis of the dppm analog. Thus, to a solution of $Ni(COD)_2$ 0.274 g (1 mmol) in THF (10 ml), dppa 0.577 g (1.5 mmol) was added. The solution turned red after 10 min. To the red solution, NiI_2 0.310 g (1 mmol) in THF (150 ml, the solubility of NiI_2 in THF is about 2.5 mg ml^{-1}) was added. The solution turned green and a dark green precipitate was formed. The volume was reduced by evaporation under vacuum to 50 ml and ether 20 ml was added. The solid was filtered off and washed with several portions (5 ml) of ether. *Anal.* Calc. for $C_{84}H_{63}I_2N_3Ni_3O_3P_6$: C, 56.73; H, 3.54; N, 2.36. Found: 56.59; H, 3.59; N, 2.42%. δ ^{31}P (298 K, toluene-d_8) δ ^{31}P 61 (s); δ ^{1}H (298 K, toluene-d_8) δ H 6.8–7.4 [m, 60H, Ph]; UV–Vis [428 nm ($\varepsilon \sim 6.3 \times 10^3$ M^{-1} cm^{-1}), 572 nm ($\varepsilon \sim 7.5 \times 10^3$ M^{-1} cm^{-1})]. 70% yield.

2.2. $[Ni_3(\mu^2\text{-dppa})_3(\mu^3\text{-I})_2]PF_6 \cdot CH_2Cl_2$ (2)

Cluster **1** 0.200 g (0.13 mmol) was dissolved in THF (200 ml) and 0.034 g (0.13 mmol) of $AgPF_6$ was added, leading to an immediate color change from green to purple corresponding to oxidation of **1** to **2**. The solution was filtered and reduced to 20 ml by evaporation under vacuum. The complex was isolated by the addition of pentane. MS [MALDI] $[Ni_3dppa_3I_2]^+$ 1585 *m/z*, $[Ni_3dppa_2I_2]$ 1200 *m/z*; UV–Vis [451 nm ($\varepsilon \sim 9.2 \times 10^3$ M^{-1} cm^{-1}); 543 nm ($\varepsilon \sim 17.2 \times 10^3$ M^{-1} cm^{-1})].

3. Results and discussion

The reaction of NiI_2 with the presumed adduct 'Ni_2dppa_3' in THF solution afforded the triangular $Ni_3dppa_3I_2$ (**1**) complex in 70% yield. Oxidation of the complex with a stoichiometric amount of $AgPF_6$ led to the monooxidized product $[Ni_3dppa_3I_2]PF_6$ (**2**) in quantitative yield. In order to elucidate the structural impact of changing the dppm ligand by dppa and how it affects electronic and chemical properties of the trinuclear clusters, **1** and **2** were characterized spectroscopically, structurally, and electrochemically.

3.1. Mass spectra

Mass spectrometry is a good source of information about the relative stability of the molecular ions in the gaseous phase. The MALDI mass spectrum of **2** (Fig. 1) shows two intense peaks at 1585 and 1200 *m/z*. The 1585 peak coincides to the molecular cation **2**. The 1200 *m/z* corresponds to the fragment $[Ni_3\{\mu^2\text{-P,P}'\text{-}HN(Ph_2P)_2\}_2(\mu\text{-I})_2]^+$, resulting from the dissociation of one of the dppa ligands, and underscoring the high stability of the Ni_3 metal core in the gas phase.

3.2. Molecular structure of 1 and 2

ORTEP diagrams and crystallographic and refinement data for complexes **1** and **2** are shown in Figs. 2 and 3 and Table 1. Complexes **1** and **2** crystallize in monoclinic $P2_1/n$ and triclinic $P\bar{1}$ space groups, respectively. The three nickel–nickel bonds in **1** and **2** are crystallographically independent with none of the nickel atoms occupying special positions [8]. The triangle of nickel atoms has two short 2.4431(10); Ni(2)–Ni(3), 2.4505(10); and one long Ni(1)–Ni(3), 2.4666(9) sides for complex **1**. Upon oxidation, complex **2** shows two long sides [Ni(1)–Ni(2), 2.4885(14), Ni(3)–Ni(1), 2.4898(14)] and one shorter [Ni(2)–Ni(3), 2.4665(14)] side. After oxidation of **1** by one electron, the average metal–metal bond length expands by 0.028 Å. Here, if it is important to underscore that the X-ray structure was collected at 100 K for **1** and at 298 K for **2**, and the significant differences in temperatures may account partly for the differences in Ni–Ni bond lengths.

The Ni–I bond distances ranged from 2.6351(8) to 2.7782(8) (Ni–I av., 2.7077(8)) for complex **1** and are slightly shorter in complex **2** (from 2.6127(12) to 2.7050(13), Ni–I av. = 2.658), suggesting antibonding character of the HOMO, with respect to Ni–I bonding (vide infra). These are very close on average, to those (Ni–I av. = 2.70 and 2.65) found in the dppm complex [4] for the neutral and oxidized forms, respectively.

Complex **1** shows Ni–P bonds shorter (ranging from 2.166(2) to 2.1820(2); Ni–P av., 2.17(2)) compared to its dppm analog [4] $[Ni_3(\mu^2\text{-dppm})_3(\mu^3\text{-I})_2]$ (ranging from 2.187(3) to 2.196(3); Ni–P av., 2.19(1)). The Ni–P bond lengths for complex **2** range from 2.202(2) to 2.232(2) and are shorter, on average, when compared to the dppm analog [2] $[Ni_3(\mu^2\text{-dppa})_3(\mu^3\text{-I})_2]CF_3SO_3$ [2.218(1)

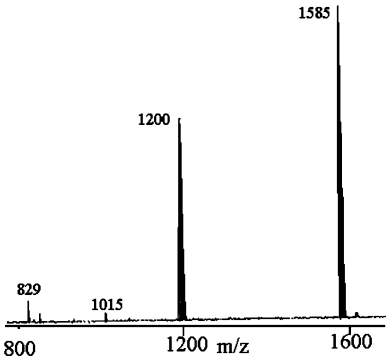

Fig. 1. MALDI mass spectrum of the complex $[Ni_3dppa_3I_2]PF_6$ (**1**).

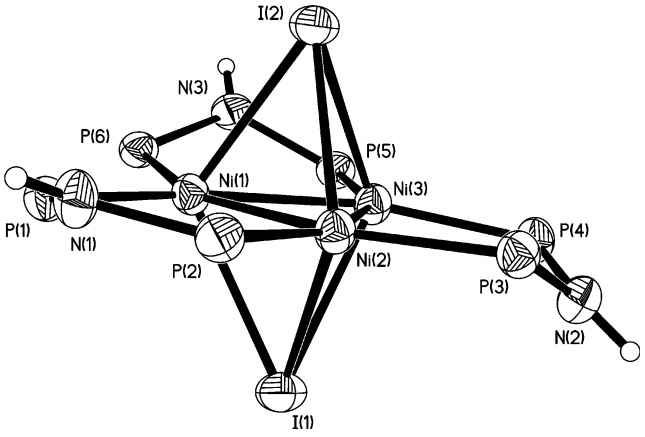

Fig. 2. ORTEP diagram (thermal ellipsoids, 50%) for complex $[Ni_3\{\mu^2\text{-}P,P'\text{-}dppa\}_3(\mu\text{-}I)_2]\cdot 2THF\cdot(CH_3)_2O$ (**1**). Selected bond length (Å) and angles (°): Ni(1)–Ni(2), 2.4431(10); Ni(2)–Ni(3), 2.4505(10); Ni(1)–Ni(3), 2.4666(9); I(1)–Ni(3), 2.6351(8); I(1)–Ni(2), 2.7782(8); Ni–I av., 2.7077(8); Ni(2)–P(3), 2.1629(16); Ni(3)–P(5), 2.1784(16); Ni–P av., 2.1731(16); P(1)–N(1), 1.693(5); P(2)–N(1), 1.688(5); P–N av. 1.690(5); P(6)–Ni(1)–P(1), 108.54(6); I(2)–Ni(1)–I(1), 117.03(3); P(1)–Ni(1)–I(1), 116.79(5); Ni(2)–Ni(1)–Ni(3), 59.88(3); Ni(2)–Ni(1)–I(1), 64.49(2); Ni(3)–Ni(1)–I(1), 60.50(2); P(3)–Ni(2)–P(2), 107.27(6); Ni(1)–Ni(2)–Ni(3), 60.54(3); P(3)–Ni(2)–I(1), 102.48(5); I(2)–Ni(2)–I(1), 114.79(3); P(4)–Ni(3)–P(5), 110.76(6); Ni(2)–Ni(3)–Ni(1), 59.58(3).

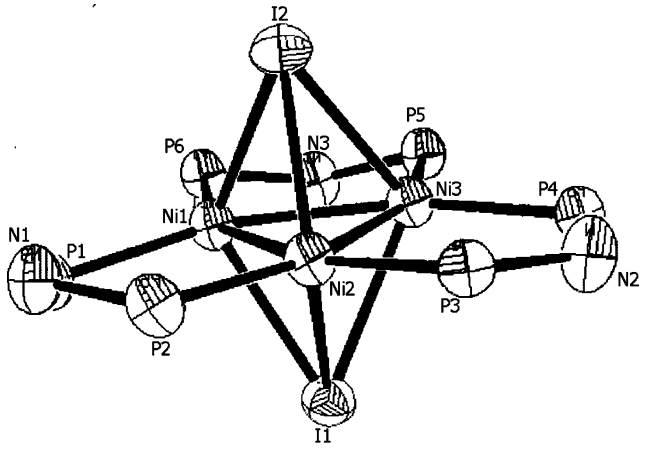

Fig. 3. ORTEP diagram (thermal ellipsoids, 50%) for complex $[Ni_3\{\mu^2\text{-}P,P'\text{-}dppa\}_3(\mu\text{-}I)_2][PF_6]$ (**2**). Selected bond length (Å) and angles (°): Ni(1)–Ni(2), 2.4885(14); Ni(2)–Ni(3), 2.4665(14); Ni(3)–Ni(1), 2.4898(14); Ni(1)–I(1), 2.6127(12); Ni(2)–I(1), 2.6977(12); Ni(3)–I(1), 2.6443(12); Ni(1)–I(2), 2.6290(12); Ni(2)–I(2), 2.6589(12); Ni(3)–I(2), 2.7050(13); Ni–I av., 2.658(5) Ni–P av., 2.218(6); P–N av., 1.689. Ni(1)–Ni(2)–Ni(3), 60.33(4); Ni(2)–Ni(1)–Ni(3), 59.40(4); Ni(1)–Ni(3)–Ni(2), 60.27(4); I(1)–Ni(1)–I(2), 117.24(4); I(1)–Ni(2)–I(2), 113.33(4); I(1)–Ni(3)–I(2), 113.56(4); P(1)–N(1)–P(2), 120.2(4); P(4)–N(2)–P(3), 123.1(4); P(6)–N(3)–P(5), 121.1(4).

vs 2.23(1). Oxidation of **1** to **2** leads to elongation of the Ni–P bonds, suggesting that the HOMO in **1** has a significant contribution from those orbitals involved also in Ni–P bonding (vide infra). Stronger metal–phosphorus interactions in the case of the dppa trimer is understandable in terms of the more accessible

Table 1
Crystallographic and refinement data for complexes $[Ni_3\{\mu^2\text{-}P,P'\text{-}dppa\}_3(\mu\text{-}I)_2]$ (**1**) and $[Ni_3\{\mu^2\text{-}P,P'\text{-}dppa\}_3(\mu\text{-}I)_2]$ $[PF_6]$ (**2**)

	1·Et_2O·2THF	**2**·CH_2Cl_2
Chemical formula	$C_{84}H_{63}I_2N_3Ni_3O_3P_6$	$C_{73}H_{65}Cl_2F_6I_2N_3Ni_3P_7$
Formula weight (g)	1778.12	1831.90
T (K)	100	296(2)
Space group	$P2_1/n$	$P\bar{1}$
a (Å)	21.7736(14)	13.836(3)
b (Å)	19.5673(13)	14.336(4)
c (Å)	21.7969(14)	19.248(5)
α (°)	90.00	84.42(2)
β (°)	118.5010(10)	84.22(5)
γ (°)	90.00	84.27(2)
V (Å^3)	8161.1(9)	3764.9(17)
Z	4	2
λ (Å)	0.71073	0.71073
ρ_{calc} (Mg m^{-3})	1.447	1.616
μ(Mo Kα) (mm^{-1})	1.607	1.842
R [a][F, $F > 4\sigma(F)$]	0.0565	0.0511
wR [b] (F^2, all reflections)	0.1337	0.12910

[a] $R(F) = \Sigma||F_o|-|F_c||/\Sigma|F_o|$.
[b] $wR(F^2) = [\Sigma[w(F_o^2-F_c^2)^2]/\Sigma w(F_o^2)^2]^{1/2}$.

phosphorus σ* orbital, due to the presence of the more electronegative nitrogen atom directly bonded to the phosphorus atom [9]. This makes the phosphine a better acceptor for dπ electron density coming from the metal centres and consequently strengthens the metal–phosphorus bonds relative to the dppm analog.

3.3. Theoretical calculations

Fig. 4 shows the HOMO and LUMO orbital diagrams for the neutral complex $[Ni_3(\mu^2\text{-}dppa)_3(\mu^2\text{-}I)_2]$.

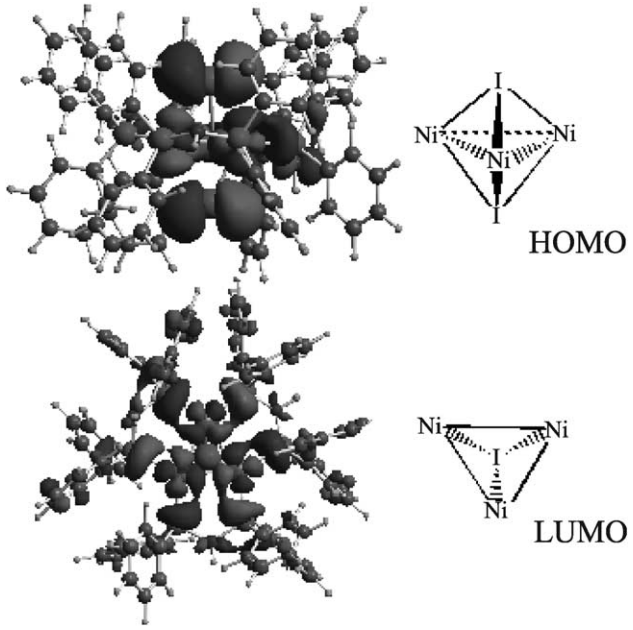

Fig. 4. The HOMO and LUMO orbital diagrams for neutral complex $[Ni_3(\mu^2\text{-}dppa)_3(\mu^2\text{-}I)_2]$ (isosurface at 0.018 au.).

The qualitative picture of the molecular orbitals does not differ substantially from that reported for the dppm analogs [6a] at the Extended Hückel calculation level. The LUMO orbital is metal-based, having the major contribution from the dπ orbitals of nickel and π orbitals of phosphorus. The main contributions to the HOMO orbital come from nickel atoms (dπ), iodine atoms (π) and phosphorus atoms (π). Partial delocalization in the plane of the nickel atoms has the effect of concentrating the electron density in the regions of the Ni–Ni bonds, Ni–P bonds and the Iodine atoms. The HOMO is antibonding respect to Ni–I bonds, having two nodal planes passing through the regions of the iodine atoms and the plane containing the Ni–I bonds. The HOMO is bonding with respect to the Ni–Ni and Ni–P bonds. The Ni–I antibonding character of the HOMO orbital and Ni–Ni and Ni–P bonding character are consistent with the shorter Ni–I distances and longer Ni–P and Ni–Ni distances of the oxidized form of the cluster.

3.4. Electrochemical studies

The electrochemistry provides evidence of the impact of substituting dppm with dppa on the electronic structure of clusters of this class. For **1**, two reversible oxidation waves $E_{1/2}(1+/0) = -1.009$ V and $E_{1/2}(2+/1+) = +0.138$ V ($\Delta E_{1/2} = 1.15$ V) are observed. As in the dppm analog [4], no reduction waves were observed at potentials as negative as -2 V vs $Cp_2Fe^{+/0}$. Under our conditions (using acetonitrile as a solvent and a $Cp_2Fe^{+/0}$ reference electrode), the $[Ni_3dppm_3I_2]$ trimer has two reversible electrochemical processes, $E_{1/2}(1+/0) = -1.090$ V and $E_{1/2}(2+/1+) = -0.150$ V ($\Delta E_{1/2} = 0.94$ V), and are slightly different from those reported in 1,1,1 trichloroethane [4]. The dppm trinuclear cluster $[Ni_3(\mu\text{-}I)_2(\mu\text{-}dppm)_3]^+$ has a slightly more negative reduction potential by 0.081 V and a more negative oxidation potential by 0.238 V compared to the dppa cluster $[Ni_3(\mu\text{-}I)_2(\mu\text{-}dppa)_3]^+$. The difference between reduction and oxidation potentials, in the case of reversible electrochemical processes, may be used to evaluate the HOMO–LUMO gap. The difference, $E_{1/2}(2+/1+) - E_{1/2}(1+/0)$, of 1.15 V in the case of the dppa clusters **1** and **2** compared to 0.94 V for dppm clusters denotes increased thermodynamic stability of the dppa $51e^-$ species compared to its dppm analog. The more positive reduction potentials for the reduction of the dppa bridged cluster **2**–**1**, compared to their dppm analogs, quantitatively reflects the increased π-acceptor character of dppa compared to dppm.

4. Supplementary material

Crystallographic data for the structural analysis have been deposited with the Cambridge Crystallographic Data Centre, CCDC Nos. 189642 and 189643. Copies of this information may be obtained free of charge from The Director, CCDC, 12 Union Road, Cambridge, CB2 1EZ, UK (fax: +44-1223-336033; e-mail: deposit@ccdc.cam.ac.uk or www: http://www.ccdc.cam.ac.uk).

Acknowledgements

Authors thank DOE (DE-FG03-99ER14992) for general support of this research.

References

[1] E. Simón-Manso, M. Valderrama, V. Arancivia, Y. Simón-Manso, D. Boys, Inorg. Chem. 39 (2000) 1650.
[2] (a) P. Bhattacharyya, D.J. Woollins, Polyhedron (1995) 3367;
(b) H. Noeth, L. Meinel, Z. Anorg. Allg. Chem. 349 (1967) 225.
[3] S. Browning, D.H. Farrar, D.C. Frankel, J.J. Vittal, Inorg. Chim. Acta 254 (1997) 329.
[4] D.A. Morgenstern, G.M. Ferrence, J. Washington, J.I. Henderson, L. Rosenhein, J.D. Heise, P.E. Fanwick, C.P. Kubiak, J. Am. Chem. Soc. 118 (1996) 2198.
[5] (a) F.T. Wang, J. Najdzionek, K.L. Leneker, H. Wasserman, D.M. Braitsh, Synth. React. Inorg. Metal-Org. Chem. 8 (1978) 119;
(b) R.A. Schunn, Inorg. Syn. 15 (1974) 5.
[6] (a) D.L. DeLaet, P.E. Fanwick, C.P. Kubiak, Organometallics 5 (1986) 1807;
(b) D.L. DeLaet, D.R. Renato, P.E. Fanwick, C.P. Kubiak, J. Am. Chem. Soc. 109 (1987) 754;
(c) J. Gong, C.P. Kubiak, Inorg. Chim. Acta 162 (1989) 19;
(d) J. Gong, C.P. Kubiak, Thesis Purdue University, 1990.
[7] J. Ellermann, W. Wend, Nouv. J. Chim. 10 (1986) 313.
[8] W. Massa, Crystal Structure Determination, 2nd ed., Springer, Berlin, 2000.
[9] A.G. Orpen, Chem. Commun. (1985) 1310.
[10] (a) A.D. Becke, J. Chem. Phys. 98 (1993) 5648;
(b) J.P. Perdew, Y. Wang, Phys. Rev., Ser. B 45 (1992) 13244;
(c) M.J. Frisch, G.W. Trucks, H.B. Schlegal, P.M.W. Gill, B.G. Johnson, M.A. Robb, J.R. Cheesman, T. Keith, G.A. Petersson, J.A. Montgomery, K. Raghavachari, M.A. Al-Laham, V.G. Zakrzewski, J.V. Ortiz, J.B. Foreman, C.Y. Peng, P.Y. Ayala, W. Chen, M.W. Wong, J.L. Andres, E.S. Replogle, R. Comperts, R.L. Martin, D.J. Fox, J.S. Binkley, D.J. Defrees, J. Baker, J.P. Strwart, M. Head-Gordon, C. Gonzalez, J.A. Pople, GAUSSIAN-94, revision B.3; Gaussian Inc., Pittsburgh, PA, 1995.